

Uniform Pores in Cross-Linked Polymers by Dispersed Fumed Silica Templating

Mariana Duarte,^{†,‡} Johan Billing,[†] Yan Liu,[†] Mats Leeman,[†] Ola J. Karlsson,^{†,§} and Ecevit Yilmaz*,[†]

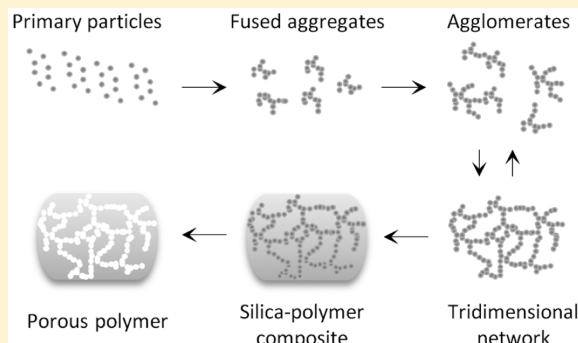
[†]MIP Technologies AB, A Subsidiary of Biotage AB, Box 737, 22007 Lund, Sweden

[‡]Department of Biomedical Engineering, Division of Nanobiotechnology, Lund University, Box 118, 22100 Lund, Sweden

[§]Physical Chemistry, Center for Chemistry and Chemical Engineering, Lund University, Box 124, 22100 Lund, Sweden

Supporting Information

ABSTRACT: Hydrophobic fumed silica dispersions in organic monomers were explored as a pore-forming system in polymer synthesis. The method developed provides a simple and effective way of controlling the pore size in highly cross-linked polymers. Fumed silica suspensions in divinylbenzene were polymerized with subsequent etching of the silica particles, therefore creating the porosity in the polymer. The resulting polymers are mesoporous materials, exhibiting an extremely narrow pore size distribution with an average pore size of about 100 Å, replicating the size of the nanofiller. BET surface areas were found appreciably high (~350 m²/g). Furthermore, the rheological behavior of the prepolymerization mixtures was studied to elucidate the formation of the porous network and showed that a tridimensional network of particles is formed at a minimum silica fraction (Φ_v) of 0.08.



INTRODUCTION

The control over polymer porosity in the preparation of cross-linked polymers has been a topic of research for several decades,¹ and new methods are constantly emerging as it remains one of the main issues in polymer synthesis.² In recent years, polymer particles have gained increasing interest as separation matrices due to their low production price and both mechanical and chemical robustness. Moreover, the endless availability of monomer systems for custom-made production of highly efficient and selective adsorbents translates into a vast pool of polymers designed for specific separation tasks. The interest in controlling porosity aspects is widely spread over a large range of applications. In separation techniques such as chromatography, a high uniformity of the pore network is of utmost importance, since it results both in a reduction of the dispersion effects and in an improved control of size exclusion phenomena.

In the most common synthesis methods for porous polymeric materials, a liquid porogen is used, and pore size control is obtained by manipulation of parameters such as porogen type, monomer-to-porogen ratio, cross-linking degree, and reaction temperature.³ Other methods for achieving results on pore control, especially in the mesoporosity range, are templating methods.⁴ In some of these methods, the voids of a solid silica material are filled with a monomer mixture, and after polymerization, the silica is removed through etching.⁵ This was first done with porous silica beads⁶ and has more recently been carried out with e.g. KIT-6 silica,⁷ colloidal crystals,⁸ and pellets of compressed fumed⁹ and colloidal silica.¹⁰ Alternatively,

dispersed templates such as colloidal silica particles have been used to create cavities in polymeric materials through a polymer–silica composite templating method.¹¹ The resulting voids corresponded to the shape of the colloidal silica particles; however, due to the fact that these particles exist in discrete form and not aggregated, a polymer with interconnected pores was not obtained. Nonetheless, Johnson et al. obtained connected porosity by compressing colloidal silica nanoparticles into pellets to create contact between the particles.¹²

In the present work, fumed silica was used as a nanofiller in a templating method to shape the porosity of polymer particles. To date, there are few reports on the use of dispersed fumed silica as a disposable pore-forming agent,¹³ and in this study it has been investigated in detail for the first time. The nanometer size and aggregation properties of fumed silica¹⁴ enable a new route to create a uniform porosity in highly cross-linked polymeric materials, as illustrated in Figure 1.

Fumed silica exists in the form of fused aggregates of primary particles with a defined size. These aggregates form larger agglomerates by hydrogen bonding of silanol groups present on the surface of the particles, and at a sufficiently high concentration of fumed silica in a determined medium, the percolation of these agglomerates provides a tridimensional network in the system.

Received: February 6, 2015

Revised: May 29, 2015

Published: June 30, 2015

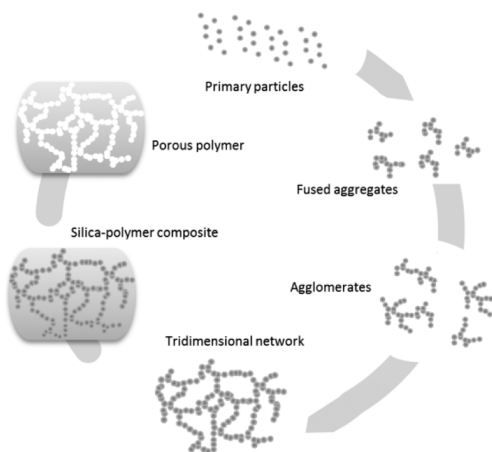


Figure 1. Schematic overview of the pore network development using fumed silica.

Controlling pore formation using dispersed sacrificial fillers or templates is dependent on the interactions between the filler particles in the polymerization medium. Thus, the controllable parameters are the composition of the medium and the concentration, size, and surface characteristics of the filler particles. Particle–particle interactions of hydrophilic silica (bare fumed silica) in a nonpolar medium are strong due to hydrogen bonding between the silanol groups, leading to very highly viscous mixtures even at low silica loadings.¹⁸ Hydrophobic (surface methylated) fumed silica was chosen in this work in order to decrease the number of silanol groups available for interaction, which results in a better particle–medium compatibility and generates a lower thickening effect at the same concentration of filler hence enabling a higher loading. While particle–particle interactions are desirable to give shape to a well-connected network of pores, it is required that high loadings of silica can be used to achieve the desired pore volume and high surface area.

EXPERIMENTAL SECTION

Synthesis of Porous Polymers. Silica–poly(divinylbenzene) composites were prepared by thermally initiated free radical polymerization in bulk, using fumed silica with a hexamethyldisilane-treated surface of an average particle size of 12 nm (Aerosil R8200, Evonik). In 20 mL glass vials, 10 g of divinylbenzene 80% grade (previously treated with aluminum oxide to remove the stabilizer) and 0.1 g of AIBN were dissolved. To this solution, different amounts of fumed silica were slowly added (0, 0.5, 1.0, 1.5, 2.0, 2.5, 3.0, 4.0, 6.0, 10, and 12 g), and the mixture was gently stirred with a spatula. The mixtures were then purged with N₂ and placed in an oven at 60 °C for approximately 16 h. After polymerization, the resulting monoliths were crushed in a mortar and the particles were sieved between 20 and 32 μm. Porous polymer particles were obtained after removal of the silica with 3 M NaOH in 40% MeOH in water. 20 mL of NaOH solution was used per gram of silica. The mixture was sonicated and then stirred for 3 days. After completion of the reaction, the polymer particles were separated from the sodium silicate in a separation funnel. The polymer particles were then washed with abundant warm water several times and finally twice with methanol before being dried in a vacuum oven at 40 °C overnight. The volume fractions of silica (Φ_v) were calculated using the density value of 2.1 g/cm³.

Material Characterization. To confirm the effective removal of the silica, FT-IR analyses were run in a PerkinElmer Spectrum 100 ATR instrument, and thermogravimetric analyses were performed in a TA Instruments Q50 Series at 20.00 °C/min. Pore volumes and surface areas were obtained by N₂ adsorption analyses which were

provided at the Department of Chemical Engineering, Chemical Centre, Lund University. The analyses were run on a Micromeritics ASAP 2400. The samples were degassed overnight at 60 °C. Viscosity data were obtained with a Visco Bohlin 88 BV from Bohlin Reologi AB. TEM micrographs were recorded by Intertek Wilton (Redcar, UK) using a Philips CM12 instrument, and sample preparation was performed using a Reichert Ultracut E ultramicrotome.

Inverse-Size Exclusion Chromatography. Because of the fact that most applications of polymer materials in separation are in liquid media, the assessment of the pore network in the wet state seemed opportune. The polymers exhibit a swelling of 40% in THF, which could influence the pore size. In order to elucidate potential differences in pore size in the dry and the wet state, inverse size-exclusion chromatography (ISEC) analyses were performed, and data were analyzed according to a method established by Halász and Martin.¹⁶ For ISEC measurements, polymer particles (20–32 μm) were packed in HPLC columns of 4.6 mm i.d. × 50 mm. In order to remove very small particles (<1 μm) and avoid possible blocking of the column frits, an extra refinement of the particle size distribution was made by sedimentation of the particles in MeOH/H₂O (80/20 v/v%). The columns were packed by a high-pressure down-fill column slurry packing procedure, using THF and an air-driven pump. The pressure was set to 200 bar, and approximately 500 mL of solvent was passed through the columns.

The experiments were run in a Shimadzu LC-10AD. Poly(styrene) standards (M_w = 162 to 2 460 000) and acetone (which was used as the void marker) were dissolved in THF. The mobile phase was THF, and the flow rate was set between 0.25 and 1 mL/min.

The calculation of the pore sizes was done using the equation

$$p_i = 0.621M_i^{0.588} \quad (1)$$

The average pore size (\bar{p}) in the polymer was calculated based on the retention volumes of the probes according to eqs 2–5:

$$\bar{p} = \sum_{i=1}^n \bar{p}_i x_i \quad (2)$$

$$x_i = K_{i+1} - K_i \quad (3)$$

$$K_i = \frac{V_i - V_0}{V_t - V_0} \quad (4)$$

$$\bar{p}_i = \frac{p_{i+1} + p_i}{2} \quad (5)$$

K_i is the permeation coefficient, V_i is the retention volume of each probe, V_t is the total liquid volume in the column, and V_0 is the void volume.

RESULTS AND DISCUSSION

The infrared absorbance of the siloxane bond—a strong peak at approximately 1080 cm⁻¹—was used to monitor silica removal (Figure 2). After etching, the peak was no longer visible, indicating essentially complete removal of silica from the polymer matrix. Thermogravimetric analyses performed on polymers produced with low (Φ_v = 0.03), medium (Φ_v = 0.09), and high (Φ_v = 0.25) loadings of silica also confirmed the removal of the inorganic filler, with remaining silica contents being lower than 1 wt % (Figure 3).

The polymers were subjected to N₂ adsorption analyses (see isotherms in the Supporting Information) and were found to be predominantly mesoporous (2–50 nm), which was also supported by inverse-size exclusion chromatography (ISEC) data (Table 1). The use of ISEC as a porosity characterization method was restricted to the samples with $\Phi_v \geq 0.08$ as polymers with less pore volume did not provide a satisfactory chromatographical resolution.

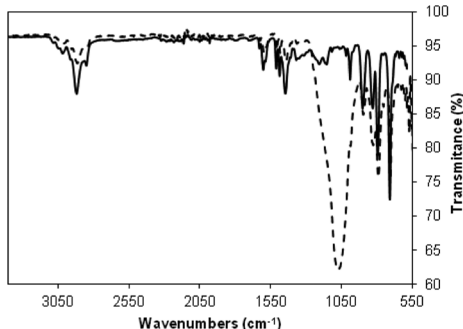


Figure 2. FT-IR spectra of silica–polymer composite at $\Phi_v = 0.08$ (dashed line) and the resulting polymer after silica etching (solid line), indicating that residuals of silica are extremely low.

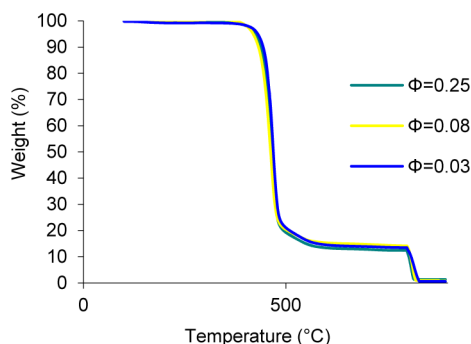


Figure 3. Thermogravimetric analyses of resulting polymers (after removal of silica) at three representative loadings of silica. At 800 °C the remaining of silica is confirmed to be less than 1 wt %.

Table 1. Average Pore Diameters by N₂ Adsorption and Inverse Size-Exclusion Chromatography (ISEC)

Φ_v	N ₂ adsorption (Å)	ISEC (Å)
0.02	66	
0.03	79	
0.05	68	
0.06	85	
0.08	99	94
0.09	79	71
0.12	90	99
0.17	100	108
0.25	107	105
0.30	110	115

Results showed that the total pore volume per gram of polymer increases proportionally with the silica content of the polymerization mixture (Figure 4A). This result supports the pore-control hypothesis of the presented method.

As the results show in Table 1, ISEC yielded only minimal differences compared to N₂ adsorption, demonstrating that the swelling does not significantly influence the pore diameter of the produced polymers. While the peak maximum in the BJH plot (Figure 6) was consistent with the size of the primary particles, the average pore diameter exhibits a small increasing trend as shown by the values in Table 1 by both analysis methods. This can be expected due to the decreasing influence of the microporosity (Figure 5), and it is not a sign that the silica is forming bigger clusters.

The BET surface area of the polymers is plotted in Figure 4B, where three stages are highlighted. It is observed a steep

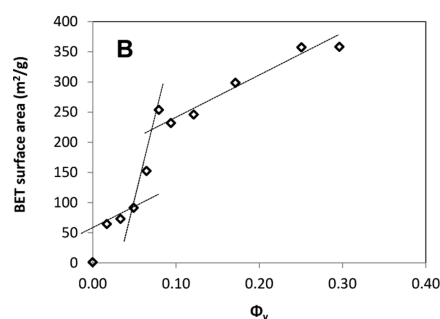
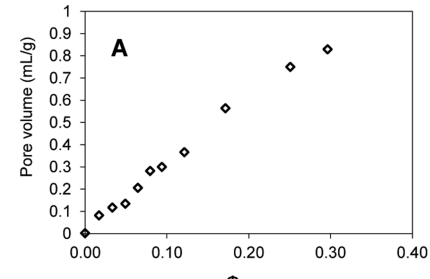


Figure 4. Total pore volume (A) and BET surface area (B) in the polymer as a function of silica loading. The lines are only intended as a guide to the eye.

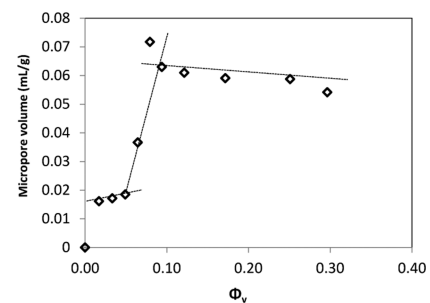


Figure 5. Micropore volume as a function of silica fraction. The lines are only intended as a guide to the eye.

increase between $\Phi_v = 0.05$ and $\Phi_v = 0.08$ that we attribute to the increase in the microporosity as seen in Figure 5. The maximum BET surface area and pore volume values are above 350 m²/g and close to 1 mL/g, respectively, which are typical values for resins used in chromatography and adsorption.

Data from micropore analysis using the *t* method with the Harkins and Jura equation are shown in Figure 5. The data show that the volume of micropores (<2 nm) ranges from 0.02 to 0.07 mL/g, depending on the silica content. Up until $\Phi_v = 0.05$, the micropore volume is about 0.02 mL/g, and then it increases sharply to 0.07 mL/g at $\Phi_v = 0.08$ where it reaches a plateau. Since the microporosity is an unavoidable result of the polymerization of DVB unrelated to the presence of silica particles, this suggests that there is a degree of mesopore connection that increasingly allows the micropores to become accessible in the N₂ adsorption analyses. Therefore, the plateau after $\Phi_v = 0.08$ represents the highest degree of network connection achieved.

The primary silica particles used in this work have an average diameter of 12 nm, and ideally they would only generate pores of about this size. As shown in Figure 6, the distribution of pore sizes in the polymers shows a constant peak shape for various Φ_v that matches well the 12 nm silica size. This indicates that the particles do not form large agglomerates or clusters, but

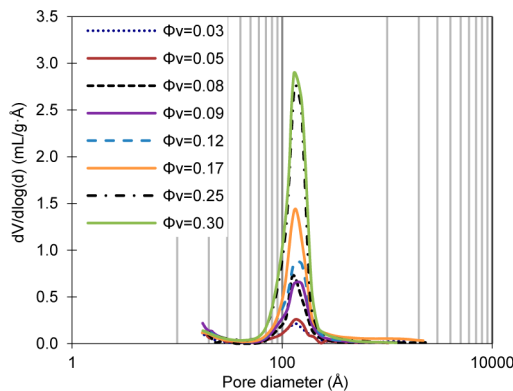


Figure 6. Pore size distribution obtained by N_2 adsorption and calculated by the BJH method applied to the desorption branch of the isotherm.

rather controlled filamentous networks consisting of single particle chains, proving full control over the pore size of the manufactured polymers.

The rheological behavior of the silica–monomer dispersions was also assessed in order to elucidate the particle–particle interactions in the medium and consequently the formation of the pore network. The interaction of agglomerates through hydrogen bonding generates a tridimensional network of connected silica particles. Under dynamic conditions, these interactions are broken, leading to the shear thinning behavior that is characteristic of silica suspensions in organic media.¹⁷

In this study, as seen in Figure 7, the shear thinning is nonexistent or very limited until approximately $\Phi_v = 0.03$

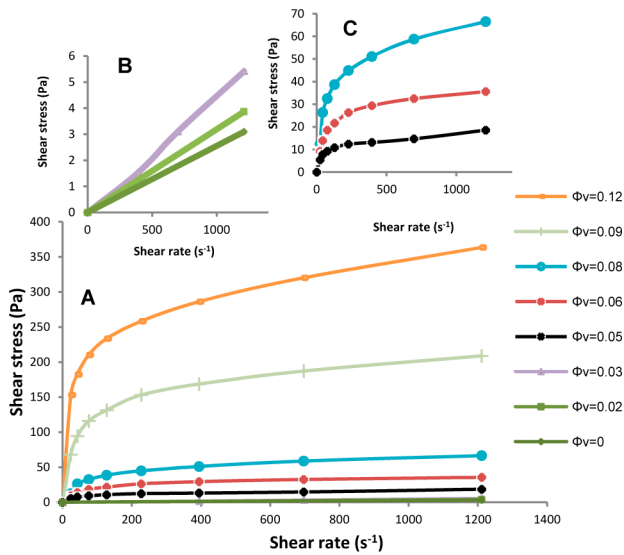


Figure 7. Rheological behavior of fumed silica suspensions in DVB under static conditions. (B) and (C) are enlarged intervals from (A).

(Figure 7B), and therefore the mixtures are characterized by a typical Newtonian behavior. This indicates that the agglomerate–agglomerate interactions are weak and that the network is poorly connected. At $\Phi_v = 0.05$, the shear thinning becomes evident (Figure 7C), suggesting some degree of percolation of the agglomerates.

The point of infinite connection of particles is known as the percolation threshold and has been reported for fumed silica suspensions to be in the range of $\Phi_v = 0.01$ to $\Phi_v = 0.033$.^{17,18}

In Figure 8 the rheological behavior of the mixtures under dynamic conditions is plotted as a frequency dependence of the

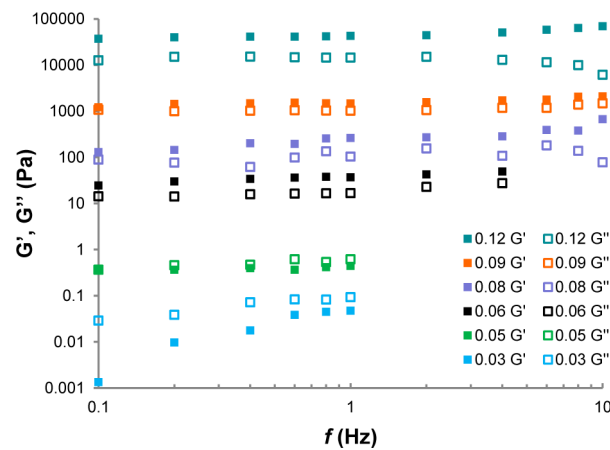


Figure 8. Storage (G') and loss (G'') modulus as a function of frequency for various silica dispersions (Φ_v from 0.03 to 0.12).

storage (G') and loss (G'') modulus. Here, the percolation threshold, i.e., the lowest concentration at which $G' > G''$, is above this range, between $\Phi_v = 0.05$ and $\Phi_v = 0.06$. The difference can be due to the hydrophobic surface modification on the used silica, as the interactions of native silica in organic medium are stronger, and therefore the percolation is achieved at lower concentration. Furthermore, this value correlates well with the hypothesis that the steep increase in the micropore volume from $\Phi_v = 0.05$ to $\Phi_v = 0.08$, observed in Figure 4A, is due to a network connection. Moreover, from $\Phi_v = 0.08$ a significantly larger increase in viscosity can be seen (Figure 7A), suggesting a higher order of agglomerate–agglomerate interactions which lead to an interconnected pore-forming structure. In light of these facts, we conclude that below $\Phi_v = 0.05$ the network formation is incomplete (leading to incomplete connectivity between the pore channels in the polymer) and above $\Phi_v = 0.05$ they gradually interconnect until at $\Phi_v = 0.08$ the full network is obtained.

The materials were investigated by TEM to visualize the structured network of fumed silica and the resulting interconnected porosity (Figure 9). In the micrographs of the composite (Figures 9A and 9B), the fumed silica network is visible as the spotted dark regions. At higher magnification (Figure 9B) the filamentous aggregation of individual fumed silica particles (approximately size 12 nm) can be seen. In the resulting polymer (Figures 9C and 9D) the pores are represented by the lighter shaded areas which have similar structure and size order as the fumed silica network.

CONCLUSIONS

This work presents a simple and effective method for controlling the porosity of polymers. By the use of a solid porogen, the creation of a well-interconnected pore network with a narrow pore size distribution was achieved, which is unique in the preparation of polymeric adsorbents. The concentration of silica in the polymerization mixture plays a crucial role, and at least $\Phi_v = 0.08$ is needed to generate a well-connected network of pores. The approach developed in this work is expected to be useful in porous polymer synthesis processes when solubility problems are found, the presence of a solvent is undesired, or the use of a sacrificial support is

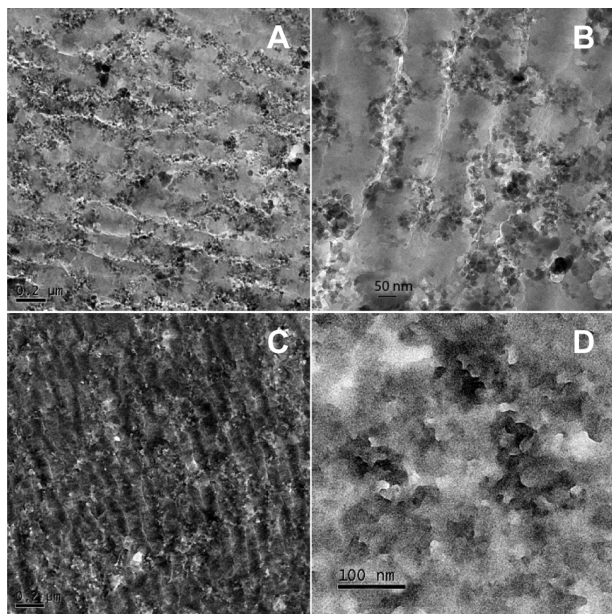


Figure 9. TEM micrographs of the DVB-fumed silica composite (A and B) and the porous polymer after etching (C and D) at $\Phi_v = 0.09$. The ridges are a result of the microtoming during the sample preparation.

convenient. The immediate fields of application in separation technology include high performance chromatography beads, molecularly imprinted polymers—where the solid porogen has vast potential for application in surface imprinting as template support—and monolithic materials with uniformly distributed mesoporosity.

ASSOCIATED CONTENT

Supporting Information

Nitrogen adsorption isotherms. The Supporting Information is available free of charge on the ACS Publications website at DOI: 10.1021/acs.macromol.5b00263.

AUTHOR INFORMATION

Corresponding Author

*E-mail ecevit.yilmaz@biotage.com (E.Y.).

Notes

The authors declare no competing financial interest.

ACKNOWLEDGMENTS

The authors acknowledge the financial support by the European Commission, under the 7th Framework programme, integrated in the PepMIP project: “Robust affinity materials for applications in proteomics and diagnostics”, grant # 264699.

REFERENCES

- (a) Sherrington, D. C. Preparation, Structure and Morphology of Polymer Supports. *Chem. Commun.* **1998**, 21, 2275–2286. (b) Wu, D.; Xu, F.; Sun, B.; Fu, R.; He, H.; Matyjaszewski, K. Design and Preparation of Porous Polymers. *Chem. Rev.* **2012**, 112 (7), 3959–4015.
- (a) Cheng, J.; Zhang, Y.; Gopalakrishnakone, P.; Chen, N. Use of the Upside-Down Method to Prepare Porous Polymer Films with Tunable Surface Pore Sizes. *Langmuir* **2008**, 25 (1), 51–54. (b) Fribe, A.; Ulbricht, M. Controlled Pore Functionalization of Poly(ethylene terephthalate) Track-Etched Membranes via Surface-Initiated Atom Transfer Radical Polymerization. *Langmuir* **2007**, 23 (20), 10316–

10322. (c) Zhu, X. X.; Banana, K.; Yen, R. Pore Size Control in Cross-Linked Polymer Resins by Reverse Micellar Imprinting. *Macromolecules* **1997**, 30 (10), 3031–3035. (d) Jiang, J.-X.; Su, F.; Trewin, A.; Wood, C. D.; Niu, H.; Jones, J. T. A.; Khimyak, Y. Z.; Cooper, A. I. Synthetic Control of the Pore Dimension and Surface Area in Conjugated Microporous Polymer and Copolymer Networks. *J. Am. Chem. Soc.* **2008**, 130 (24), 7710–7720. (e) Coutinho, F. M. B.; Teixeira, V. G.; Barbosa, C. C. R. Synthesis and Characterization of Styrene–Divinylbenzene Loaded with Di(2-ethylhexyl)phosphonic Acid. I. Influence of Diluent Mixture on the Porous Structure of the Copolymer. *J. Appl. Polym. Sci.* **1998**, 67 (5), 781–787. (f) Hasegawa, J.; Kanamori, K.; Nakanishi, K.; Hanada, T.; Yamago, S. Pore Formation in Poly(divinylbenzene) Networks Derived from Organotellurium-Mediated Living Radical Polymerization. *Macromolecules* **2009**, 42 (4), 1270–1277.

(3) (a) Svec, F.; Frechet, J. M. J. Temperature, a Simple and Efficient Tool for the Control of Pore Size Distribution in Macroporous Polymers. *Macromolecules* **1995**, 28 (22), 7580–7582. (b) Svec, F.; Frechet, J. M. J. Kinetic Control of Pore Formation in Macroporous Polymers. Formation of “Molded” Porous Materials with High Flow Characteristics for Separations or Catalysis. *Chem. Mater.* **1995**, 7 (4), 707–715. (c) Okay, O. Macroporous copolymer networks. *Prog. Polym. Sci.* **2000**, 25 (6), 711–779.

(4) Thomas, A.; Goettmann, F.; Antonietti, M. Hard Templates for Soft Materials: Creating Nanostructured Organic Materials. *Chem. Mater.* **2008**, 20 (3), 738–755.

(5) (a) Zhang, X.; Yan, W.; Yang, H.; Liu, B.; Li, H. Gaseous Infiltration Method for Preparation of Three-Dimensionally Ordered Macroporous Polyethylene. *Polymer* **2008**, 49 (25), 5446–5451. (b) Wang, Y.; Caruso, F. Template Synthesis of Stimuli-Responsive Nanoporous Polymer-Based Spheres via Sequential Assembly. *Chem. Mater.* **2006**, 18 (17), 4089–4100. (c) Yilmaz, E.; Haupt, K.; Mosbach, K. The Use of Immobilized Templates—A New Approach in Molecular Imprinting. *Angew. Chem., Int. Ed.* **2000**, 39 (12), 2115–2118. (d) Wang, Y.; Yu, A.; Caruso, F. Nanoporous Polyelectrolyte Spheres Prepared by Sequentially Coating Sacrificial Mesoporous Silica Spheres. *Angew. Chem., Int. Ed.* **2005**, 44 (19), 2888–2892.

(6) (a) Feibusch, B.; Li, N.-H. Porous Rigid Resins and Process of Preparation. US4933372 A, 1990. (b) Yilmaz, E.; Ramstrom, O.; Möller, P.; Sanchez, D.; Mosbach, K. A Facile Method for Preparing Molecularly Imprinted Polymer Spheres Using Spherical Silica Templates. *J. Mater. Chem.* **2002**, 12 (5), 1577–1581.

(7) (a) Choi, D.-H.; Ryoo, R. Template Synthesis of Ordered Mesoporous Organic Polymeric Materials Using Hydrophobic Silylated KIT-6 Mesoporous Silica. *J. Mater. Chem.* **2010**, 20 (26), 5544–5550. (b) Wu, Z.; Meng, Y.; Zhao, D. Nanocasting Fabrication of Ordered Mesoporous Phenol–Formaldehyde Resins with Various Structures and Their Adsorption Performances for Basic Organic Compounds. *Microporous Mesoporous Mater.* **2010**, 128 (1–3), 165–179.

(8) (a) Velev, O. D.; Kaler, E. W. Structured Porous Materials via Colloidal Crystal Templating: From Inorganic Oxides to Metals. *Adv. Mater.* **2000**, 12 (7), 531–534. (b) Stein, A.; Li, F.; Denny, N. R. Morphological Control in Colloidal Crystal Templating of Inverse Opals, Hierarchical Structures, and Shaped Particles. *Chem. Mater.* **2007**, 20 (3), 649–666. (c) Hu, X.; An, Q.; Li, G.; Tao, S.; Liu, J. Imprinted Photonic Polymers for Chiral Recognition. *Angew. Chem., Int. Ed.* **2006**, 45 (48), 8145–8148.

(9) (a) Weber, J.; Bergström, L. Impact of Cross-Linking Density and Glassy Chain Dynamics on Pore Stability in Mesoporous Poly(styrene). *Macromolecules* **2009**, 42 (21), 8234–8240. (b) Weber, J.; Bergström, L. Mesoporous Hydrogels: Revealing Reversible Porosity by Cryoporometry, X-ray Scattering, and Gas Adsorption. *Langmuir* **2010**, 26 (12), 10158–10164.

(10) Wilke, A.; Weber, J. Mesoporous Polymer Networks—Ultraporous DVB Resins by Hard-Templating of Close-Packed Silica Spheres. *Macromol. Rapid Commun.* **2012**, 33 (9), 785–790.

- (11) Jang, J.; Lim, B. Selective Fabrication of Carbon Nanocapsules and Mesocellular Foams by Surface-Modified Colloidal Silica Templating. *Adv. Mater.* **2002**, *14* (19), 1390–1393.
- (12) Johnson, S. A.; Ollivier, P. J.; Mallouk, T. E. Ordered Mesoporous Polymers of Tunable Pore Size from Colloidal Silica Templates. *Science* **1999**, *283* (5404), 963–965.
- (13) (a) Derylo-Marczewska, A.; Goworek, J.; Zgrajka, W. Studies of Melamine–Formaldehyde Resins by Sorption from Gas and Liquid Phases. *Langmuir* **2001**, *17* (21), 6518–6523. (b) Yilmaz, E.; Billing, J. Methods for Making Polymer Beads. US 8481603 B2, 2005.
- (14) Khan, S. A.; Zoeller, N. J. Dynamic Rheological Behavior of Flocculated Fumed Silica Suspensions. *J. Rheol.* **1993**, *37* (6), 1225–1235.
- (15) Barthel, H. Surface Interactions of Dimethylsiloxy Group-Modified Fumed Silica. *Colloids Surf., A* **1995**, *101* (2–3), 217–226.
- (16) Halász, I.; Martin, K. Pore Sizes of Solids. *Angew. Chem., Int. Ed. Engl.* **1978**, *17* (12), 901–908.
- (17) Paquien, J.-N.; Galy, J.; Gérard, J.-F.; Pouchelon, A. Rheological Studies of Fumed Silica–Polydimethylsiloxane Suspensions. *Colloids Surf., A* **2005**, *260* (1–3), 165–172.
- (18) Cassagnau, P. Melt Rheology of Organoclay and Fumed Silica Nanocomposites. *Polymer* **2008**, *49* (9), 2183–2196.